ELSEVIER

Journal of Nuclear Materials 281 (2000) 208–212

journal of nuclear materials

www.elsevier.nl/locate/jnucmat

Effect of silicon impurities and heat treatment on uranium hydriding rates

A.L. DeMint *, J.H. Leckey

Development Division, Oak Ridge Y-12 Plant, P.O. Box 2009, Bldg. 9202, MS 8096, Oak Ridge, TN 37831-8096, USA

Received 2 December 1999; accepted 9 June 2000

Abstract

Several experiments were run to identify variables that affect the hydriding rate of depleted uranium. Only two factors affecting hydriding rate were found: temperature (and time) of the final heat treatment, and silicon content. Increasing the time and temperature of alpha-phase anneals increased the reaction rate, and annealing in the beta-phase greatly increased the reaction rate over alpha-phase annealing. Silicon contents of up to 100 wppm cause dramatic increases in the hydride reaction rate for both alpha- and beta-phase annealed samples. © 2000 Elsevier Science B.V. All rights reserved.

PACS: 81.05.Bx; 81.40.Ef; 82.30−b; 82.20.Pm

1. Introduction

The reaction of hydrogen with uranium is important for many reasons. In particular, in moisture- and oxygen-free systems, ambient hydrogen can lead to pitting, which destroys the surface finish of precisely machined surfaces and disrupts joining features. After pitting initiation, the reaction spreads across the surface of the material, then proceeds through massive uranium at an accelerated linear reaction rate [1]. The reaction proceeds by molecular hydrogen dissociation at the uranium surface to hydrogen atoms. The formation of uranium hydride is then described by an equation that accounts for the simultaneous diffusion and reactivity of the hydrogen atoms. In any given region, once the fraction converted to uranium hydride becomes significant, the reaction front spalls due to internal stresses arising from the expansion accompanying the formation of uranium hydride, and exposes fresh uranium to the hydrogen gas. While uranium has a density of 18.9 g/cm^3, uranium hydride's density is only 11.4 g/cm^3. The overall reaction stoichiometry is

$$2U_{(S)} + 3H_{2(G)} \rightarrow 2UH_{3(S)}. \qquad (1)$$

The reaction rate is very sensitive to many parameters, including material processing, surface condition, and impurities in the metal [2–4]. One common impurity in uranium is the element silicon. This report describes a study that evaluates the effect of silicon concentration on the reaction rate of hydrogen with uranium. This effect of silicon is studied as it correlates with uranium heat-treating operations involving intermediate annealing, swaging schedules, phase (alpha or beta) of the material during annealing, as well as the time and temperature profile of the final anneal.

2. Experimental methods

Material from a high-purity ^{238}U billet (billet A) was processed into samples in several different ways to determine which processing variables affected the hydriding rate. The fabrication process involved the swaging of bar stock from ~20 to 3.18 mm diameter with two intermediate anneals, followed by vacuum heat treating in either the beta or high-alpha range. Rods cut from plate

---

* Corresponding author. Tel.: +1-865 574 1801; fax: +1-865 574 2582.

E-mail address: azd@y12.doe.gov (A.L. DeMint).

0022-3115/00/$ - see front matter © 2000 Elsevier Science B.V. All rights reserved.
PII: S0022-3115(00)00238-5

rolled to 6.35 mm were also swaged to 3.18 mm; these samples required no intermediate anneals. Swaging schedules and the time and temperature of the intermediate anneals were systematically varied according to a statistical experimental design. Table 1 shows the processing schedule for these samples. Samples were cleaned in a nitric acid solution before the hydriding test to remove any oxides and surface oils that could hinder the reaction.

Chemistry variables were also studied by processing samples from different lots of uranium and comparing hydriding rates. Table 2 shows the trace impurity levels in each billet.

The technique chosen for studying the reactivity to hydrogen was the one Powell used for high-precision kinetics work [1,5]. The hydriding apparatus consisted of two sealed chambers, one with a known pressure of hydrogen and the other with the uranium sample inside, evacuated. The chamber with the uranium sample was heated to a specified temperature (200°C) and held at that temperature while hydrogen was admitted from the pressurized chamber. The initial hydrogen pressure over the sample was typically 8000 Torr and the final pressure was typically 5000 Torr. Hydrogen uptake was determined by measuring the pressure drop in the pressurized tank corrected for the amount of hydrogen in the reaction chamber at the end of the run, from which could be determined the amount of hydrogen the sample consumed.

3. Experimental results

From the hydrogen pressure drop as a function of time, the extent of the reaction in terms of uranium hydride stoichiometry was calculated using the ideal gas law, sample weight and Eq. (1). A representative hydriding reaction run (alpha annealed with 28 ppm silicon) is shown in Fig. 1 by the open black circles. A chemical reaction can be characterized in many ways. The one chosen in this section is the time to complete 97% of the overall reaction. The next section uses an alternative method of analyzing the reaction rate data.

Table 1
Processing variable table for samples from billet A[a]

Starting size (mm)	Swaging reduction per pass (%)	Intermediate anneal temperature (°C)	Final heat treatment time (h)	Final heat treatment temperature (°C)	Hydriding time (s)
20	10	600	1.0	740	1980, 1950, 1980
20	10	615	4.0	655	2700
20	10	615	4.0	655	2760
20	10	615	0.5	600	3390
20	10	615	0.5	600	3300
20	10	650	0.5	655	2610
20	10	650	0.5	655	2670
20	20	650	4.0	600	3150
20	20	650	4.0	600	3120, 2970
6.35	10	n/a	4.0	600	3090
6.35	10	n/a	4.0	600	3150
6.35	20	n/a	4.0	655	2580
6.35	10	n/a	4.0	655	2610
6.35	10	n/a	0.5	600	3300

[a] In some cases, multiple samples were hydrided to determine variability.

Table 2
Trace impurity levels (wppm) in three uranium billets[a]

	Billet A	Billet B	Billet C
Al	7	8	13
C	30	30	54
Cr	<2	<2	3
Cu	9	10	7
Fe	<10	18	<10
Mn	15	15	5
Ni	14	14	6
Si	28	17	88
Ti	6	9	<4

[a] Carbon content was determined by the Leco method, the other elements were determined by emission spectroscopy.

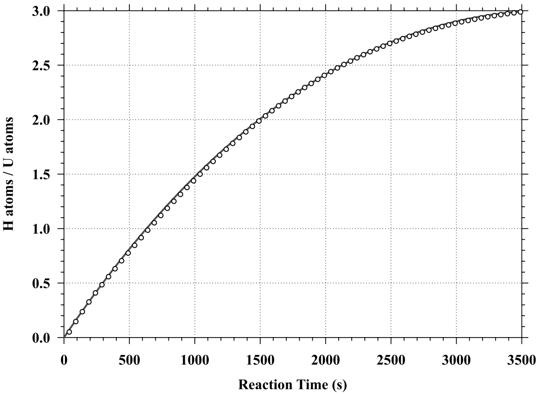

Fig. 1. Typical reaction run showing extent of reaction versus reaction time. Open circles represent experimental data. The solid line represents the best fit of the data for this run to the uranium hydriding model described in this paper, using a spall fraction parameter value of 0.956.

Table 3 presents reaction times (here defined as the time for the hydriding reaction to proceed to 97% UH_3 stoichiometry) for the samples made from billet A (see Table 1), grouped by final heat treatment. A sample with no heat treatment is also included in this table. The hydriding rate was determined for multiple samples of the same material in two instances to establish variability. As can be seen from Table 3, the only factors found to affect the hydriding rate were the temperature and time of the final anneal. Samples hydrided extremely slowly in the cold-worked condition (no anneal); samples hydrided faster after a high-alpha-phase anneal (655°C) than after a low-alpha-phase anneal (600°C); and samples that were annealed in the beta range (740°C) hydrided fastest of all. With the alpha-annealed samples, increasing the hold time at temperature increased the hydriding rate for the 600°C anneal but did not noticeably affect the hydriding rate for samples annealed at 655°C.

Insufficient studies were done to confirm a time–temperature relationship in beta-annealed samples, but it appears as though simply entering the beta region produces a sample that hydrides rapidly, and time or temperature of the hold may not be as important.

Samples made from billet C reacted considerably faster than those made from billets A or B and processed identically. Alpha-annealed samples from billet C heat treated at 655°C for 4 h reacted in an average of 1700 s, whereas material from billets A and B averaged nearly 2700 s and 2800 s, respectively. The material from billet C reacted faster than even beta-annealed material from billet A (average 1970 s). A comparison of the chemistries of the three billets shows silicon levels to be an obvious difference: silicon levels are low in billets A and B (28 and 17 wppm, respectively), and moderate in billet C (88 wppm). While the concentrations of other impurities varied among the billets, their levels and absolute variability were lower than that for silicon.

To determine whether silicon does in fact affect the hydriding rate, another set of samples was prepared with silicon contents ranging up to 300 wppm. Fig. 2 shows the time-dependence of a number of runs as a function of alpha- and beta-annealed conditions, as well as silicon

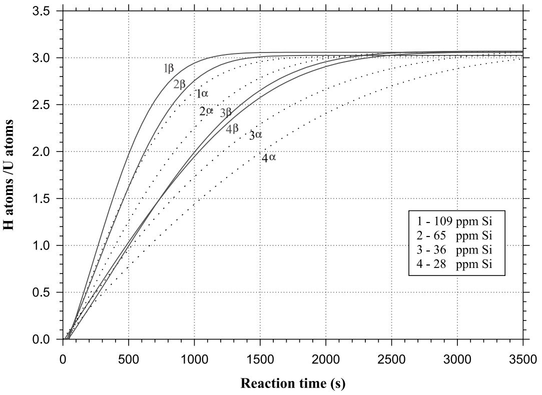

Fig. 2. The time dependence of a series of runs showing that increased amounts of silicon increase the reaction rate. Also shown is the increased reaction rate for β-annealed material (solid lines) as compared with α-annealed material (dashed lines) of the same silicon content. All α-annealed samples were annealed for 4 h.

Table 3
Heat treatment time–temperature conditions for samples from billet A[a]

	740°C–1 h (β-phase)	655°C–4 h (α-phase)	655°C–0.5 h (α-phase)	600°C–4 h (α-phase)	600°C–0.5 h (α-phase)	No heat treatment
	1980	2700	2610	3150	3390	>18,000
	1950	2760	2670	3120	3300	
	1980	2580		2970	3300	
		2610		3090		
				3150		
Average	1970	2663	2640	3096	3330	>18,000

[a] The values in the table are the times in seconds to complete 97% of the overall reaction.

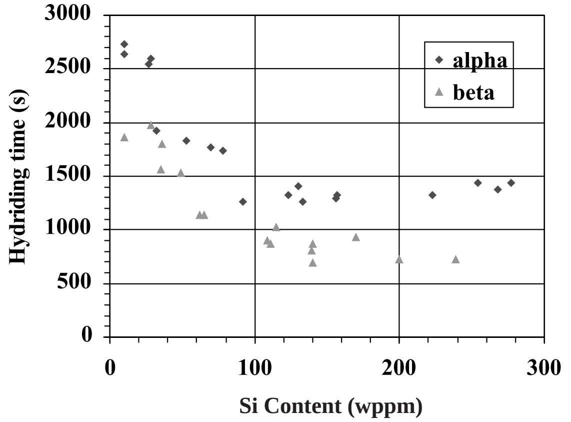

Fig. 3. The reaction rate dependence for both silicon content and anneal phase over a large number of runs is shown.

content. When the hydriding time is plotted as a function of silicon content, the effect of silicon on the hydriding rate can clearly be seen (Fig. 3). Reaction time drops sharply with increasing silicon until the silicon content reaches ~100 wppm, where the curve begins to level off. The curve for beta-annealed samples parallels the curve for alpha-annealed samples but is shifted down by ~400 s: the increase in reaction rate gained by adding silicon is independent of heat treatment.

It is postulated that beta-annealed material has less internal stresses, and therefore hydrides more quickly. Table 3 shows that uranium in the cold-worked condition (no heat treatment) hydrides very slowly, showing that increased retained internal stresses slow hydriding. Vandermeer [6] states that uranium generates internal stresses when thermally cycled in the alpha-phase (due to its anisotropy of both thermal expansion and elastic modulus). Those stresses could slow hydriding compared to beta-annealed material, which has been subjected to the dimensional change associated with heating and cooling only once (as the material was cooled from the beta-phase).

4. Hydriding reaction model

The hydriding rate data were analyzed in more detail using the linear hydriding model described by Kirkpatrick and Condon [7]. Using this model, the hydriding rate equation can be put in the form

$$\frac{dq}{dt} = -vA\rho/M, \tag{2}$$

where q is the quantity of uranium reacted in moles, t time, v the reacting front velocity, A the surface area of the reacting front, ρ the density of uranium (18.9 g/cm^3), and M is the molecular weight of uranium (238 g/mol).

The reacting front velocity is given by

$$v = \frac{1}{t_I}\left(\frac{D_E}{akU_C}\right)^{1/2}, \tag{3}$$

where t_I is the time of the initial spall, D_E the generalized diffusion coefficient of hydrogen through uranium, a the ratio of hydrogen atoms to uranium atoms in uranium hydride (three), k the reaction rate constant for the reaction of hydrogen atoms with uranium, and U_C is the mole fraction of uranium at which spalling begins to occur.

The time of the initial spall can be expressed in terms of more fundamental parameters as

$$t_I = \frac{-\ln(U_C)}{kC_0}, \tag{4}$$

where C_0 is the equilibrium solubility of hydrogen in uranium in units of mole fraction at the reaction temperature. The solubility can be expressed as

$$C_0 = \frac{N \times 4.183 \times 10^{-6}\exp(-894/T)p^{1/2}}{N + 4.183 \times 10^{-6}\exp(-894/T)p^{1/2}}, \tag{5}$$

where T is the temperature of the specimen in Kelvin and p is the hydrogen pressure in Pa.

The parameter N represents the maximum transient, super-equilibrium concentration of free hydrogen atoms in the metal lattice and is given by

$$N = \exp(-2.362 - 2305/T). \tag{6}$$

The diffusion coefficient of hydrogen through uranium, D_E, in units of M^2/s, is given by

$$D_E = 1.9 \times 10^{-6}\exp(-5280/T)\left(\frac{N}{N - C_0}\right)^{1/2}. \tag{7}$$

The expression for the reaction rate constant k is given in units of 1/s by

$$k = 10.4\exp(1592/T). \tag{8}$$

In order to solve Eqs. (2)–(8), it is first necessary to express the surface area (A) and the pressure (p) in terms of the quantity of unreacted uranium remaining (q). For this study, the relationship between the quantity of uranium reacted and the pressure is

$$p = p_0 - \frac{3RT_g(q_0 - q)}{2V}, \tag{9}$$

where p_0 is the initial pressure in the hydriding volume, R the gas constant, T_g the temperature of the gas, q_0 the initial quantity of uranium, and V is the free volume of the hydrogen gas.

For the cylindrical specimen used in this study, the radius is much smaller than the length and the surface area of unreacted material can be approximated by

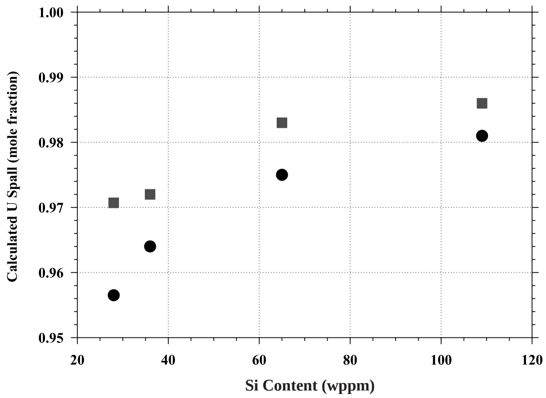

Fig. 4. Relationship between fraction of uranium required to be reacted before spalling occurs and silicon content of material in weight parts per million. The α-annealed material appears as circles; the β-annealed material squares.

$$A = \left(\frac{4\pi hMq}{\rho}\right)^{1/2}, \tag{10}$$

where h is the length of the cylinder.

This forms a set of equations that is best solved numerically as an initial value problem. The solution algorithm begins by using Eqs. (2)–(8) at the reaction temperature, with the initial pressure and surface area to predict the amount of uranium reacted over a finite time step. Based on this result, a new pressure and a new surface area are calculated using Eqs. (9) and (10), respectively. The new pressure and new surface area are then used iteratively in Eqs. (2)–(8) to step forward in time, until no more uranium remains. The time-dependence of the reaction of the uranium is converted to the time-dependence of the stoichiometry of uranium hydride formation using Eq. (1).

5. Hydriding rate data analysis

The model described in the previous section does not explicitly account for the effects of either silicon impurities or heat treatment on the reaction rate. For the data analysis, U_C (the mole fraction of uranium at which spalling begins) was used as an adjustable parameter in the model. The solid line in Fig. 1 shows the fit of a typical run to the model, using U_C as the sole adjustable parameter. The best fit for this run requires a value of U_C of 0.9565. Fig. 4 shows the best fit value of U_C for each of the runs shown in Fig. 2.

By way of comparison, a value for U_C of 0.978 is reported in for material with a silicon content of 60 ppm [8].

6. Conclusions

The hydriding rate of uranium is dramatically increased by the presence of trace amounts (∼100 wppm) of silicon. Although other interpretations of this effect are possible, the effect is consistent with additional silicon causing spalling to occur at higher values of the mole fraction of uranium (decreasing the mole fraction of uranium hydride required to spall). Apparently, the silicon impurities disrupt the lattice sufficiently to promote spalling.

The hydriding rate is affected to a lesser degree by varying the final heat treatment: samples annealed in the beta-phase react more quickly than those annealed in the alpha, and increasing the temperature (and to some extent the time) of an alpha-phase anneal also increases the hydriding rate. Although differences in hydriding rates have sometimes been attributed to material hardness, we feel the hardness is an indication of residual stresses in the material and as such directly related to heat treatment.

References

[1] G.L. Powell, W.L. Harper, J.R. Kirkpatrick, J. Less Common Met. 116 (1991) 172.
[2] J. Bloch, M.H. Mintz, J. Less Common Met. 166 (1990) 241.
[3] J. Bloch et al., Z. Phys. Chem., N.F. 164 (1989) 1193.
[4] E. Swissa et al., J. Nucl. Mater. 173 (1990) 87.
[5] G.L. Powell, Z. Phys. Chem., N.F. 164 (1989) 1227.
[6] R.A. Vandermeer, in: Metallurgical Technology of Uranium and Uranium Alloys, vol. 1, Physical Metallurgy of Uranium and Uranium Alloys, Transcripts of a seminar on the state-of-the-art, Gatlinburg, TN, USA, 26–28 May 1981, American Society for Metals, Metals Park, OH, 1982.
[7] J.R. Kirkpatrick, J.B. Condon, J. Less Common Met. (1991) 172.
[8] J.B. Condon, J. Phys. Chem. 79 (1975) 392.